Universality of subleading corrections for self-avoiding walks in the presence of one-dimensional defects

1997 J. Phys. A: Math. Gen. 30 4939

(http://iopscience.iop.org/0305-4470/30/14/009)

J. Phys. A: Math. Gen. **30** (1997) 4939–4961. Printed in the UK PII: S0305-4470(97)82245-7

Universality of subleading corrections for self-avoiding walks in the presence of one-dimensional defects

Sergio Caracciolo†‖, Maria Serena Causo‡¶ and Andrea Pelissetto§+

† Scuola Normale Superiore and INFN–Sezione di Pisa, I-56100 Pisa, Italy
‡ Dipartimento di Fisica and INFN–Sezione di Lecce, Università degli Studi di Lecce, I-73100 Lecce, Italy
§ Dipartimento di Fisica and INFN–Sezione di Pisa, Università degli Studi di Pisa, I-56100 Pisa, Italy

Received 3 March 1997

Abstract. We study three-dimensional self-avoiding walks in the presence of a one-dimensional excluded region. We show the appearance of a universal subleading exponent which is independent of the particular shape and symmetries of the excluded region. A classical argument provides the estimate: $\Delta = 2\nu - 1 \approx 0.175(1)$. The numerical simulation gives $\Delta = 0.18(2)$.

1. Introduction

An important problem in statistical mechanics is the study of the critical behaviour of systems in geometries with boundaries. One usually considers situations in which the geometric constraint changes the critical behaviour: in the renormalization-group terminology these are the cases in which the boundary is a *relevant* perturbation. However, there are also cases, as the one we are concerned with in this paper, in which the leading critical behaviour is unchanged and the presence of the boundary appears as an *irrelevant* perturbation.

Maybe it is due to their name that the role of *irrelevant* operators is generally not well studied. Indeed, by definition, they do not modify the fixed point of the renormalization-group transformations. In particular they do not change the values of the critical exponents and manifest themselves only through subleading corrections to the fixed-point Hamiltonian. Nonetheless, in any actual computation the fixed-point Hamiltonian is replaced by an effective Hamiltonian whose parameters are tuned closed to criticality. This means that as soon as a precise determination of the universal scaling behaviour is needed, it becomes important to also have good control on the terms responsible for corrections to scaling.

In this paper, we will concentrate on three-dimensional self-avoiding walks (SAWs) in the presence of an excluded one-dimensional region. We will extend the results of [1–3] which showed the appearance of a new critical exponent $\Delta \approx 0.22$ for the case of a half-line. Here we will consider more general one-dimensional regions and we will show that the value of Δ is independent of the shape and symmetries of the excluded region: only

‖ E-mail address: Sergio.Caracciolo@sns.it
¶ E-mail address: causo@le.infn.it
+ E-mail address: pelisset@ibmth.difi.unipi.it

0305-4470/97/144939+23$19.50

the dimensionality plays a role. Moreover, we will show that Δ can be predicted to a very good accuracy by a purely geometrical argument.

This paper is organized as follows. In section 2 we give a general discussion of the relevance of the perturbation introduced by the excluded region and we give a prediction for the subleading exponent. In section 3 we describe the geometries that we analyse and the choice of observables which allow the easiest and most precise determination of Δ. In section 4 we give a few details of the simulation, while in section 5 we give the final results. Appendix A presents the computation of the generating function for ordinary random walks in the presence of excluded hyperplanes which allow a direct check of the results of section 2. An analogous computation for the case of a single excluded point and for an excluded needle is reported in [1]. Appendix B contains some unrelated results on the small-momentum behaviour of the two-point function.

2. Excluded set and corrections to scaling

In the terminology of the field-theoretic approach to critical phenomena, the critical behaviour of the SAW is governed by the fixed point of the $O(n)$ σ-model analytically continued to $n = 0$ [4–9]. The presence of an excluded region corresponds to a perturbation due to the introduction of an operator which creates vacancies in the $O(n)$ model. Now consider the correlation function† between a spin at the origin and one in the bulk at location $\boldsymbol{r}$; this function will have the scaling form

$$G_{\mathcal{R}}(\boldsymbol{r};\beta) \sim r^{-(d-2+\eta_{\mathcal{R}})} F_{\mathcal{R}}(\boldsymbol{r}/\xi(\beta)) + r^{-(d-2+\eta'_{\mathcal{R}})} F'_{\mathcal{R}}(\boldsymbol{r}/\xi(\beta)) + \cdots . \tag{2}$$

Here β is the inverse temperature, and $\xi \sim (\beta_c - \beta)^{-\nu}$ is the correlation length *in the unperturbed theory*; the critical inverse temperature β_c and the exponent ν are *not* modified by the presence of the vacancies, unless the excluded region $\mathcal{R}$ is so big that the remaining set $\mathbb{Z}^d \setminus \mathcal{R}$ is effectively a space of lower dimensionality. See [10] to see how thin a set has to be before $\mu = 1/\beta_c$ changes. However, the behaviour of the other quantities depends on whether the perturbation is relevant or irrelevant [11].

(a) If the perturbation is *relevant*, then the leading spin–spin decay exponent $\eta_{\mathcal{R}}$ *differs* from its bulk value η (and as a consequence the leading susceptibility exponent $\gamma_{\mathcal{R}} = (2 - \eta_{\mathcal{R}})\nu$ differs from its bulk value $\gamma = (2 - \eta)\nu$). Likewise, the leading scaling function $F_{\mathcal{R}}$ differs from its bulk value F; in particular, it has a non-trivial angular dependence [12].

(b) If the perturbation is *irrelevant*, then $\eta_{\mathcal{R}}$ and $F_{\mathcal{R}}$ are *unchanged* from their bulk values η and F. In particular, the leading scaling function F has *no angular dependence*. The effects of the perturbation show up only in the *non-leading* exponents and scaling functions $\eta'_{\mathcal{R}}, \ldots$ and $F'_{\mathcal{R}}, \ldots$, which *can* differ from their bulk values.

In either case, $\eta_{\mathcal{R}}$ and $F_{\mathcal{R}}$ (and indeed all of the exponents $\eta'_{\mathcal{R}}, \ldots$ and scaling functions $F'_{\mathcal{R}}, \ldots$ except for an unknown amplitude) are universal in the sense that they depend only on the *global* properties of the excluded region $\mathcal{R}$, such as its dimensionality.

More subtle is the case in which the perturbation is marginal: $\eta_{\mathcal{R}}$ is equal to the bulk value but the universal scaling behaviour may be broken by logarithmic violations and observables associated to the perturbation can show a complete breaking of universality, in

† In the SAW language we have

$$G_{\mathcal{R}}(\boldsymbol{r};\beta) = \sum_{N=0}^{\infty} \beta^N c_{N,\mathcal{R}}(\boldsymbol{r}) \tag{1}$$

where $c_{N,\mathcal{R}}(\boldsymbol{r})$ is the number of SAWs going from 0 to $\boldsymbol{r}$ in N steps without intersecting the region $\mathcal{R}$.

the sense that they can have critical exponent with an explicit dependence from the coupling of the perturbation [13, 14].

To understand the effect of the introduction of the excluded region we must thus understand if the perturbation is relevant or irrelevant. We will resort to a geometric argument. Consider in a d-dimensional space a set E and let $d(E)$ denote the number of dimensions in which the set E extends to infinity. Let us now recall the fundamental rule in geometric probability for the dimension of the generic intersection $A \cap B$ of two geometric sets A and B which are immersed in a space of d dimensions:

$$d(A \cap B) = d(A) + d(B) - d. \tag{3}$$

A negative sign of $d(A \cap B)$ means that A and B do not generically intersect in dimension d outside any bounded volume. The application of (3) extends also to random geometries where one considers a probability measure on a configuration space which is concentrated on a set of events with given Hausdorff dimension.

For example, the generic intersection of two ordinary random walks, which have Hausdorff dimension 2, has dimension $4 - d$, and thus they do not generically intersect in $d > 4$. By using the well known random-walk representation of the Euclidean $O(n)$-vector field theory [15, 16, 8], for which the interaction is concentrated on the intersections among walks, it is then possible to understand why for $d > 4$ in the critical region only a trivial theory is recovered: simply because the walks intersect almost nowhere! We can say that for $d > 4$:

(a) the probability of intersections of two random walks in the critical region scales towards its limiting value with the correlation length as ξ^{4-d};

(b) critical indices take their free-field (that is mean-field) values, the interaction term in the Hamiltonian is *irrelevant* and induces only subleading corrections.

In $d = 4$ the interaction becomes *marginal* and is responsible only for logarithmic corrections to the critical indices [7]. It is said that 4 is the upper critical dimension of the model.

In $d < 4$ the interaction is *relevant* and thus it changes the critical indices.

Similar ideas have been used to discuss the critical behaviour of gauge theories and random surfaces, see for example [17].

Let us now consider the case of walks in the presence of an excluded region $\mathcal{R}$ of dimension $d_{\mathcal{R}}$. Consider first ordinary random walks whose Hausdorff dimension is two. Then the dimension of a generic intersection with the region $\mathcal{R}$ of dimension $d_{\mathcal{R}}$ is

$$d_{\text{int}} = 2 + d_{\mathcal{R}} - d. \tag{4}$$

The previous argument suggests the following cases:

- $d_{\mathcal{R}} = 0$: this is the case in which we are excluding only a finite set of lattice sites. The upper critical dimension (with its logarithmic corrections) is $d = 2$;
- $d_{\mathcal{R}} = 1$: this is the case in which we are excluding a finite set of one-dimensional lines. The upper critical dimension (with its logarithmic corrections) is $d = 3$.

Formula (4) can also be obtained from other considerations [1]. If $\mathcal{R}$ is a $d_{\mathcal{R}}$-dimensional hyperplane, consider the projection of the walk on $\mathcal{R}'$, the orthogonal complement of $\mathcal{R}$. Also the projection is a random walk. The probability of intersection will then be the probability of first return to the point $\mathcal{R} \cap \mathcal{R}'$. But the probability that a $\overline{d}$-dimensional random walk eventually passes through a point scales as $1/N^{\overline{d}/2-1}$ if $\overline{d} > 2$, while it is one if $\overline{d} \leqslant 2$. Since in our case $\overline{d} = d - d_{\mathcal{R}}$, we see that for $d_{\text{int}} \geqslant 0$ the walk generically intersects the region $\mathcal{R}$, while for $d_{\text{int}} < 0$ the probability vanishes as $1/N^{-d_{\text{int}}/2}$, in agreement with our argument. Finally notice that when $d_{\mathcal{R}} = d - 1$, one can apply the results for the

so-called vicious walkers. Indeed the behaviour of d one-dimensional vicious walkers† can be viewed as the behaviour of a d-dimensional walker in a space bounded by $d(d-1)/2$ $(d-1)$-dimensional hyperplanes [18, 19].

Let us now arrive at the case of SAW. Their Hausdorff dimension is $1/\nu$ (see for example [7, appendix B]). For the dimension of a generic intersection with the region $\mathcal{R}$ we obtain

$$d_{\rm int} = \frac{1}{\nu} + d_{\mathcal{R}} - d. \tag{5}$$

Let us consider again a series of cases, remembering that for $d \leqslant 4$ according to the Flory formula $\nu \approx 3/(d+2)$, which is exact in $d = 1, 2$, must be corrected by logarithmic violations in $d = 4$, and is a good approximation in $d = 3$.

• $d_{\mathcal{R}} = 0$: excluded points are a relevant perturbation only if $d \leqslant 1/\nu$, that is in $d = 1$. We remark that the subcase in which the excluded set consists of a single point $\mathcal{R} = \mathcal{P}$, when $\mathcal{P}$ is chosen to be a nearest neighbour of the origin of the walk, can be mapped into a problem *without* vacancies. Indeed each walk of N steps, starting from the origin, can be seen as a walk of $N+1$ steps starting from $\mathcal{P}$ whose first step is the previous origin. Under this mapping the asymmetry induced by the exclusion of $\mathcal{P}$ can be seen as the correlation between the position of the endpoint of the walk with the direction of the first step.

• $d_{\mathcal{R}} = 1$: in $d = 1, 2$ the perturbation is relevant, but it is already irrelevant in $d = 3$.

Thus in $d = 3$ with a finite set $\mathcal{R}$ of excluded lines, we expect that, regardless of their disposition is space, the probability that a walk intersects the region $\mathcal{R}$ scales as $\xi^{2-1/\nu}$, or, since $\xi \sim N^{\nu}$, as $N^{2\nu-1}$.

In the field-theoretic language this dimensional argument implies in (2)

$$\eta' = \eta - d_{\rm int} = \eta + 2 - \frac{1}{\nu}. \tag{6}$$

Consequently, if $P_k(x)$ is a homogeneous polynomial of degree k in the coordinates of the endpoint of the walk, we have

$$\langle P_k(x) \rangle_{N,\mathcal{R}} = N^{k\nu} \left(A(k) + \frac{B_{\mathcal{R}}(k)}{N^{\Delta}} + \cdots \right) \tag{7}$$

where $\langle \cdot \rangle_{N,\mathcal{R}}$ is the average in the ensemble of walks of length N that do not intersect $\mathcal{R}$ and Δ a subleading exponent. If (6) holds, we have

$$\Delta = -d_{\rm int}\nu = 2\nu - 1. \tag{8}$$

In general we expect renormalization effects to change (6) and thus (8) introducing an anomalous dimension. However, experience with three-dimensional models indicates that these corrections, if not vanishing, are extremely small and thus we expect (8) to be in any case a very good approximation.

The amplitude $A(k)$ is not universal, because of an unknown scale factor, but it should not depend on the excluded region. Moreover, since in the critical limit the distribution of the endpoint is rotationally symmetric, $A(k)$ vanishes whenever $\int \mathrm{d}\Omega_x \, P_k(x) = 0$ where $\mathrm{d}\Omega_x$ is the normalized measure on the sphere S^{d-1}. This suggests a very convenient way to compute the subleading exponent Δ induced by the introduction of the excluded region. The idea is to consider observables which have zero expectation value in the rotationally invariant continuum limit and which do not vanish under the residual discrete symmetry that the lattice has after the introduction of the excluded region. For these quantities $A(k) = 0$ so that the leading term scales as $N^{k\nu-\Delta}$ which makes the determination of Δ much easier.

† Related works on vicious walkers can be found in [20, 21].

Let us notice that in all this discussion we have always assumed that the first subleading exponent is related to the introduction of the excluded region. This is true for those quantities for which $\langle P_k(x)\rangle$ would vanish in the absence of the excluded region, i.e. for those $P_k(x)$ which are not only non-rotationally invariant but which are also not symmetric under the transformations of the cubic group. If instead $\langle P_k(x)\rangle$ would not vanish even in the absence of the excluded region, it is not clear *a priori* which exponent should show up first. For cubic-symmetric $P_k(x)$ for which $A(k) = 0$ an extensive analysis [22, 23] shows that in the absence of any excluded region

$$\langle P_k(x)\rangle \sim N^{k\nu-\Delta_{\rm latt}} \tag{9}$$

with $\Delta_{\rm latt} \approx 2\nu$. For $d = 3$ this exponent is much larger than (8) and thus, in the presence of an excluded region, we expect all non-rotationally invariant $P_k(x)$ to behave as $N^{k\nu-\Delta}$ with Δ given by (8). We should also mention that the exponent Δ defined here is unrelated to the exponent $\omega\nu \approx 0.5$ which controls the leading confluent correction for SAWs in the absence of any excluded region and which has been the object of much attention in literature [24–27].

3. The models

We have concentrated upon the problem of three-dimensional SAWs starting from the origin in the presence of an excluded region $\mathcal{R}$ which consists of a finite collection of half-lines—we will call them '*needles*'—along the coordinate axes.

For this purpose we have studied the following cases (see figure 1) for the region $\mathcal{R}$ (for a reason to be clarified later all the needles start from a site whose distance from the origin is two: for example the needle along the positive z-axis will start from the site with coordinate $(0, 0, 2)$):

(1) a needle along one direction;
(2) two needles along the positive and negative directions of an axis;
(3) two needles along two different axes;
(4) four needles in a plane along the two directions of two axes;
(5) three needles along three different axes;
(6) six needles along the two directions of all the three axes.

Notice that in the last case it is necessary that the needles start from a point located at distance two from the origin, otherwise the SAW starting from the origin would necessarily touch one of the needles.

Let us now define a few observables which will allow us to study the effect of the introduction of the excluded region. If (x, y, z) are the coordinates of the endpoint of the SAW (or, equivalently, (r, θ, ϕ) in polar coordinates) a natural choice of observables is given by $r^l Y_{l,m}(\theta, \phi)$, $l \neq 0$, where $Y_{l,m}(\theta, \phi)$ are the spherical harmonics. If $\langle r^l Y_{l,m}(\theta, \phi)\rangle$ is not identically vanishing because of the residual cubic symmetry which survives the introduction of the excluded region, this quantity is a natural candidate for a direct determination of the exponent Δ. Indeed, since the critical limit is rotational-invariant, the leading term for $N \to \infty$, i.e. $A(k)$ in formula (7), will vanish and thus this quantity will scale as $N^{l\nu-\Delta}$.

Let us now classify the various observables according to the value of l. For $l = 1$ the possibilities are

$$r(Y_{1,1}(\theta, \phi) + Y_{1,-1}(\theta, \phi)) \sim x \tag{10}$$

$$r(Y_{1,1}(\theta, \phi) - Y_{1,-1}(\theta, \phi)) \sim y \tag{11}$$

$$rY_{1,0}(\theta, \phi) \sim z. \tag{12}$$

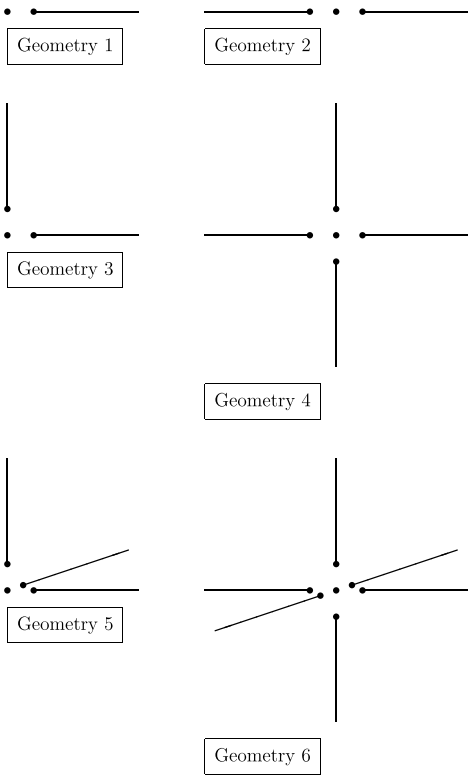

Figure 1. The six different geometries we have simulated. For each geometry we have reported, as a dot, the starting point of the walk (located at the origin) and the starting points of the excluded needles (located at distance two from the origin).

We can thus define $O_1(x) = x$ and the obvious permutations. This observable is useful whenever the region $\mathcal{R}$ is not invariant under the inversion of the x-axis.

Let us now consider $l = 2$. In this case we have

$$r^2(Y_{2,2}(\theta,\phi) + Y_{2,-2}(\theta,\phi)) \sim x^2 - y^2 \tag{13}$$

$$r^2(Y_{2,2}(\theta,\phi) - Y_{2,-2}(\theta,\phi)) \sim xy \tag{14}$$

$$r^2(Y_{2,1}(\theta,\phi) + Y_{2,-1}(\theta,\phi)) \sim xz \tag{15}$$

$$r^2(Y_{2,1}(\theta,\phi) - Y_{2,-1}(\theta,\phi)) \sim yz \tag{16}$$

$$r^2 Y_{2,0}(\theta,\phi) \sim x^2 + y^2 - 2z^2. \tag{17}$$

We can thus define three observables

$$O_{2,1}(x,y) = x^2 - y^2 \tag{18}$$

$$O_{2,2}(x,y) = xy \tag{19}$$

$$O_{2,3}(x,y) = z^2 - \tfrac{1}{2}(x^2 + y^2). \tag{20}$$

It is clear that, whenever a symmetry between two axes exists, the two variables $O_{2,1}$ and $O_{2,3}$ are equivalent. In our calculation we have thus only considered the last two quantities.

Finally, we have considered $l = 4$. In this case many different observables can be defined. We have only considered

$$O_{4,1} = \tfrac{2}{3}[x^4 + y^4 + z^4 - 3(x^2y^2 + x^2z^2 + y^2z^2)] \tag{21}$$

$$O_{4,2}(x) = x^4 + \tfrac{1}{2}(y^4 + z^4) - 3x^2(y^2 + z^2). \tag{22}$$

Notice that when the excluded region is symmetric under any exchange of two axes $O_{4,1}$ and $O_{4,2}$ are equivalent. It is also worth remarking that $O_{4,1}$ and $O_{4,2}$ do not vanish even in the absence of any excluded region, as they are invariant under the full cubic group.

Let us now define exactly our observables for the various geometries:

(1) geometry 1 (needle along the positive x-axis): we measure $O_1 \equiv O_1(x)$, $O_2 \equiv O_{2,3}(y, z)$ and $O_4 \equiv O_{4,2}(x)$;

(2) geometry 2 (two needles along the x-axis): we measure $O_2 \equiv O_{2,3}(y, z)$ and $O_4 \equiv O_{4,2}(x)$;

(3) geometry 3 (two needles along the positive x- and y-axis): we measure $O_1 \equiv \frac{1}{2}(O_1(x) + O_1(y))$, $O_2 \equiv \frac{1}{2}(O_{2,3}(y, z) + O_{2,3}(z, x)) = -\frac{1}{2}O_{2,3}(x, y)$, $\tilde{O}_2 \equiv O_{2,2}(x, y)$ and $O_4 \equiv O_{4,1}$;

(4) geometry 4 (four needles in the xy-plane): we measure $O_2 \equiv \frac{1}{2}(O_{2,3}(y, z) + O_{2,3}(z, x)) = -\frac{1}{2}O_{2,3}(x, y)$ and $O_4 \equiv \frac{1}{2}(O_{4,2}(x) + O_{4,2}(y))$;

(5) geometry 5 (three needles along three different axes): we measure $O_1 \equiv \frac{1}{3}(O_1(x) + O_1(y) + O_1(z))$, $\tilde{O}_2 \equiv \frac{1}{3}(O_{2,2}(x, y) + O_{2,2}(x, z) + O_{2,2}(x, y))$ and $O_4 \equiv O_{4,1}$;

(6) geometry 6 (six needles): we measure $O_4 \equiv O_{4,1}$.

4. The Monte Carlo simulation

4.1. Monte Carlo observables

The purpose of our simulation was to compute the mean values of the observables we have defined in the previous section in the presence of an excluded region $\mathcal{R}$. A direct strategy would be to simulate SAWs in the presence of the region $\mathcal{R}$ and then to compute the mean values of the various observables in the usual way. However, this strategy requires different simulations for different excluded regions $\mathcal{R}$. To avoid repeating the runs many times we have simulated SAWs without any excluded region and then we have reweighted the results in order to obtain the mean values of interest. Since, as we have previously discussed, the introduction of the excluded region is an irrelevant perturbation, this strategy does not introduce any significant loss of efficiency.

Let us suppose that we want to compute $\langle \mathcal{O} \rangle_{N,\mathcal{R}}$ where $\langle \cdot \rangle_{N,\mathcal{R}}$ indicates the ensemble of SAWs of length N that do not intersect the region $\mathcal{R}$. Then we simply use

$$\langle \mathcal{O} \rangle_{N,\mathcal{R}} = \frac{\langle \mathcal{O}\theta^{(\mathcal{R})} \rangle_N}{\langle \theta^{(\mathcal{R})} \rangle_N} \tag{23}$$

where $\langle \cdot \rangle_N$ indicates the average in the ensemble of all SAWs of length N and $\theta^{\mathcal{R}}$ is an observable which assumes the value one if a walk does not intersect $\mathcal{R}$ and zero otherwise. Notice moreover that $\langle \theta^{(\mathcal{R})} \rangle_N$ also gives the probability $p_{\mathcal{R}}$ that a SAW intersects the excluded region as $p_{\mathcal{R}} = 1 - \langle \theta^{(\mathcal{R})} \rangle_N$.

We have used (23) to obtain from our simulation the mean values $\langle \mathcal{O} \rangle_{N,\mathcal{R}}$: indeed it is enough, beside measuring at each Monte Carlo step i the value $\mathcal{O}_i$, to record $\theta_i^{(\mathcal{R})}$ which assumes the value one if the walk intersects $\mathcal{R}$, zero otherwise and then estimate $\langle \mathcal{O} \rangle_{N,\mathcal{R}}$ by

$$\frac{\sum_{i=1}^{n} \mathcal{O}_i \theta_i^{(\mathcal{R})}}{\sum_{i=1}^{n} \theta_i^{(\mathcal{R})}}. \tag{24}$$

In order to further reduce the variance of our estimates we have also symmetrized our observables. To clarify the method, suppose we want to compute $\langle O_1\rangle_{N,\mathcal{R}}$ for geometry 1 ($\mathcal{R}$ is the positive x-axis). We could consider

$$\frac{\langle x\theta^{(+x)}\rangle_N}{\langle\theta^{(+x)}\rangle_N}. \tag{25}$$

A symmetrized alternative is

$$\frac{\langle x(\theta^{(+x)}-\theta^{(-x)})+y(\theta^{(+y)}-\theta^{(-y)})+z(\theta^{(+z)}-\theta^{(-z)})\rangle_N}{\langle\theta^{(+x)}+\theta^{(-x)}+\theta^{(+y)}+\theta^{(-y)}+\theta^{(+z)}+\theta^{(-z)}\rangle_N}. \tag{26}$$

It is obvious that this quantity has the same mean value of the previous one. However, this symmetrization reduces the error on the estimates essentially at no computational cost. Indeed, since we study all six geometries at the same time, we must check in any case if the walk intersects any of the axes.

In general, given a geometry $\mathcal{R}$ we have considered all the possible sets $s_\mathcal{R}$ of excluded needles which can be obtained by all the transformations of the cubic group (six for geometry 1, three for geometry 2, 12 for geometry 3, three for geometry 4, eight for geometry 5, one for geometry 6). To each region $s_\mathcal{R}$ we associate a variable $\theta^{(s_\mathcal{R})}$, which is one if the walk does not intersect the set $s_\mathcal{R}$, zero otherwise and $O^{(s_\mathcal{R})}$ which is the suitably transformed variable. Then we compute $\langle O\rangle_{N,\mathcal{R}}$ from

$$\langle O\rangle_{N,\mathcal{R}}=\frac{\langle\sum_{\{s_\mathcal{R}\}}\theta^{(s_\mathcal{R})}O^{(s_\mathcal{R})}\rangle}{\langle\sum_{\{s_\mathcal{R}\}}\theta^{(s_\mathcal{R})}\rangle}. \tag{27}$$

The symmetrization has a large effect on the static variances of the various observables. For instance, consider for each geometry the ratio

$$R=\frac{\text{var }\theta^{\mathcal{R}}}{\text{var }\frac{1}{n_\mathcal{R}}\sum\theta^{(s_\mathcal{R})}} \tag{28}$$

where 'var' indicates the static variance and $n_\mathcal{R}$ is the number of terms in the sum. We find $R=6.6,\ 3.2,\ 3.8,\ 2.7,\ 1.8,\ 1$ in the six geometries, which represents a considerable improvement. The improvement on the error bars is, however, not so large as the symmetrized observables are more correlated than the unsymmetrized ones. Thus the error bars are only 20–30% better.

To conclude, let us comment briefly on the determination of the error bars. From a Monte Carlo run of n iterations we have estimated $\langle O\rangle_{N,\mathcal{R}}$ using

$$\langle O\rangle_{N,\mathcal{R}}=\frac{\overline{\sum_{\{s_\mathcal{R}\}}\theta^{(s_\mathcal{R})}O^{(s_\mathcal{R})}}}{\overline{\sum_{\{s_\mathcal{R}\}}\theta^{(s_\mathcal{R})}}} \tag{29}$$

where, as usual $\overline{\mathcal{O}}=\frac{1}{n}\sum_i\mathcal{O}_i$. To compute the error bars one must take into account the correlation between the numerator and the denominator: the independent error formula indeed overestimates the true error bar. For O_1 the difference is about 20–30%, for O_2 and $\tilde{O}_2$ it is 4–7%, while for O_4 the difference is negligible. We have thus used the following relation, valid in the large sample limit,

$$\text{Var}\left(\frac{\overline{\sum_{\{s_\mathcal{R}\}}\theta^{(s_\mathcal{R})}O^{(s_\mathcal{R})}}}{\overline{\sum_{\{s_\mathcal{R}\}}\theta^{(s_\mathcal{R})}}}\right)=\frac{\langle\sum_{\{s_\mathcal{R}\}}\theta^{(s_\mathcal{R})}O^{(s_\mathcal{R})}\rangle^2}{\langle\sum_{\{s_\mathcal{R}\}}\theta^{(s_\mathcal{R})}\rangle^2}\text{Var}(\mathcal{A}) \tag{30}$$

where $\mathcal{A}$ is given by

$$\mathcal{A}=\frac{\sum_{\{s_\mathcal{R}\}}\theta^{(s_\mathcal{R})}O^{(s_\mathcal{R})}}{\langle\sum_{\{s_\mathcal{R}\}}\theta^{(s_\mathcal{R})}O^{(s_\mathcal{R})}\rangle}-\frac{\sum_{\{s_\mathcal{R}\}}\theta^{(s_\mathcal{R})}}{\langle\sum_{\{s_\mathcal{R}\}}\theta^{(s_\mathcal{R})}\rangle}. \tag{31}$$

The variance of $\mathcal{A}$ has been computed using the standard techniques of autocorrelation analysis [28, 27]. Since the autocorrelation function has a very long tail (due to the fact that $\tau_{\rm exp} \sim N/f \gg \tau_{{\rm int},X}$ where f is the acceptance fraction of the algorithm and X a generic *global* observable), the self-consistent windowing method proposed in [28] does not work. Indeed even using a large window of $40\tau_{{\rm int},\mathcal{A}}$, the autocorrelation time is largely underestimated. To obtain a reliable estimate of $\tau_{\rm int}$ we have used the method proposed in [27, appendix]. We compute $\tau_{{\rm int},X}$ by

$$\tau'_{{\rm int},X}(M) = \tfrac{1}{2} + \sum_{t=1}^{M} \rho_X(t) \tag{32}$$

$$\tau_{{\rm int},X} = \tau'_{{\rm int},X}(M) + \rho_X(M) M \log\left(\frac{N}{Mf}\right) \tag{33}$$

where $\rho_X(t)$ is the normalized autocorrelation function, N the length of the walk, f the acceptance fraction; M is determined self-consistently and is the smallest integer such that $20\tau'_{{\rm int},X}(M) > M$. We have checked the *ad hoc* definition (33) in the case of ordinary random walks for which exact results are available [28]: the error in the estimation of the tail turns out to be at most 10%. We have thus set the error bars on the autocorrelation times adding to the error in the determination of $\tau'_{{\rm int},X}(M)$, one tenth of the last term in (33).

4.2. The algorithm

We have simulated SAWs of fixed length N in three dimensions without any excluded region $\mathcal{R}$. The walk is given by $N+1$ lattice points $\{\omega_i\}$, $i = 0, \ldots, N$, and always starts from the origin, i.e. $\omega_0 = 0$. Since all our observables are completely symmetric under the cubic group, it is not restrictive to fix the first step; we have chosen $\omega_1 = (1, 0, 0)$.

The simulation used the *pivot* algorithm [29, 30, 28]. In the standard implementation a site ω_k in the walk and an element g of the lattice symmetry group are chosen randomly, with uniform probability. The proposed configuration, obtained from the actual one by applying g to the part of the walk subsequent to ω_k, is accepted whenever self-avoiding. This algorithm is extraordinarily efficient for the study of global observables such as, for example, the endpoint position; indeed, the integrated autocorrelation time for these observables grows with the number N of steps in the walk like N^p, where $p \approx 0.11$ in $d = 3$, while the CPU time to produce an independent walk scales like N which is the optimal situation.

Table 1. Autocorrelation times for the pivot algorithm and our improvement for the observables O_1 (in the geometries where it does not vanish) and $p_{\mathcal{R}}$. Here $N = 1000$.

Geometry	Observable	Standard pivot $\tau_{\rm int}$	Improved pivot $\tau_{\rm int}$
1	O_1	6.92 ± 0.23	1.4869 ± 0.0030
	$p_{\mathcal{R}}$	282 ± 60	5.381 ± 0.013
2	$p_{\mathcal{R}}$	280 ± 60	5.026 ± 0.011
3	O_1	7.73 ± 0.27	1.4946 ± 0.0030
	$p_{\mathcal{R}}$	307 ± 68	5.081 ± 0.012
4	$p_{\mathcal{R}}$	311 ± 69	4.2485 ± 0.0083
5	O_1	8.58 ± 0.32	1.4293 ± 0.0029
	$p_{\mathcal{R}}$	312 ± 70	4.628 ± 0.010
6	$p_{\mathcal{R}}$	261 ± 53	2.7910 ± 0.0048

Table 2. Number of iterations.

	500	1000	2000	4000	8000	16 000	32 000
N_{iter}	3×10^7	5×10^7	6×10^7	7×10^7	1×10^8	5×10^7	2×10^7

Table 3. One excluded needle. Here CL denotes the confidence level of the fit.

	Geometry 1				
	Cut	$\langle O\rangle \pm \delta\langle O\rangle$	$\sigma \pm \delta\sigma$	CL	
O_1	500	-1.5259 ± 0.0014	$0.400\,44 \pm 0.000\,44$	9×10^{-7}%	$\nu - \Delta =$
	1 000	-2.0229 ± 0.0018	$0.398\,31 \pm 0.000\,60$	0.114%	$1 - \nu =$
	2 000	-2.6751 ± 0.0028	$0.395\,84 \pm 0.000\,91$	14.118%	0.4123 ± 0.0006
	4 000	-3.5322 ± 0.0044	$0.393\,2 \pm 0.001\,6$	62.627%	
	8 000	-4.6324 ± 0.0060	$0.395\,5 \pm 0.002\,9$	92.618%	
	16 000	-6.092 ± 0.015	$0.396\,2 \pm 0.008\,0$		
	32 000	-8.018 ± 0.040			
O_2	500	-20.457 ± 0.047	$0.978\,13 \pm 0.000\,98$	29×10^{-4}%	$2\nu - \Delta = 1$
	1 000	-39.944 ± 0.089	$0.981\,8 \pm 0.001\,3$	3.622%	
	2 000	-78.25 ± 0.20	$0.985\,9 \pm 0.002\,0$	53.836%	
	4 000	-155.00 ± 0.43	$0.986\,6 \pm 0.003\,1$	35.367%	
	8 000	-306.42 ± 0.85	$0.990\,8 \pm 0.005\,4$	26.964%	
	16 000	-606.0 ± 3.0	1.005 ± 0.014		
	32 000	-1217 ± 10			
O_4	500	$(-110 \pm 11) \times 10^2$	2.277 ± 0.035	15.228%	$4\nu - \Delta =$
	1 000	$(-596 \pm 50) \times 10^2$	2.239 ± 0.044	20.112%	$1 + 2\nu =$
	2 000	$(-295 \pm 25) \times 10^3$	2.182 ± 0.063	22.338%	2.1754 ± 0.0012
	4 000	$(-160 \pm 12) \times 10^4$	2.056 ± 0.096	51.065%	
	8 000	$(-642 \pm 53) \times 10^4$	2.10 ± 0.20	25.931%	
	16 000	$(-304 \pm 41) \times 10^5$	1.43 ± 0.62		
	32 000	$(-82 \pm 34) \times 10^6$			

However, in our case not all the observables are of a global character: an example is the probability of intersection $p_{\mathcal{R}}$. Indeed, as can be seen from table 1, already at $N = 1000$, $\tau_{\text{int},p_{\mathcal{R}}} \approx 300$. It is easy to understand the origin of these autocorrelation times: indeed suppose the walk intersects $\mathcal{R}$ and let α be the smallest integer such that $\omega_\alpha \in \mathcal{R}$. Then all subsequent walks in the simulation will also intersect $\mathcal{R}$ at least until a successful pivot move at point i with $i < \alpha$ is performed. The probability of such a move is $\alpha f/N$ where f is the acceptance fraction. Now the problem is that the typical α is very small: if one considers the set of walks that intersect at least one of the six needles of the geometry 6, the mean value of the smallest α such that $\omega_\alpha \in \mathcal{R}$ is ≈ 13, with very small N-dependent corrections. Thus, a rough estimate of the autocorrelation times should be $N/(13f)$. For $N = 1000$ we have $f \approx 0.45$ so that we expect $\tau \approx 200$ which is indeed the order of magnitude we find. Moreover, we expect τ to increase as $N^{\approx 1}$ as it should for local observables. Indeed, we find that τ for $p_{\mathcal{R}}$ increases as N^p with $p \approx 0.9$ except in the case of geometry 6 where we observe $p \approx 0.6$, which could, however, well be an effective exponent in the region $500 \leqslant N \leqslant 32\,000$.

The other observables, such as O_1, are instead of a more global character and indeed

Table 4. Two opposite needles. Here CL denotes the confidence level of the fit.

	Geometry 2				
	Cut	$\langle O\rangle \pm \delta\langle O\rangle$	$\sigma \pm \delta\sigma$	CL	
O_2	500	-45.97 ± 0.11	0.9622 ± 0.0010	22×10^{-5}%	$2\nu - \Delta = 1$
	1 000	-88.71 ± 0.20	0.9664 ± 0.0014	1.206%	
	2 000	-171.86 ± 0.46	0.9712 ± 0.0021	32.894%	
	4 000	-336.7 ± 1.0	0.9732 ± 0.0034	23.052%	
	8 000	-658.2 ± 2.0	0.9801 ± 0.0060	33.624%	
	16 000	-1292.7 ± 6.9	0.994 ± 0.016		
	32 000	-2575 ± 25			
O_4	500	$(-299 \pm 12) \times 10^2$	2.206 ± 0.015	11.869%	$4\nu - \Delta =$
	1 000	$(-1437 \pm 50) \times 10^2$	2.190 ± 0.019	14.368%	$1 + 2\nu =$
	2 000	$(-670 \pm 25) \times 10^3$	2.162 ± 0.028	15.761%	2.1754 ± 0.0012
	4 000	$(-328 \pm 12) \times 10^4$	2.099 ± 0.045	39.275%	
	8 000	$(-1374 \pm 54) \times 10^4$	2.122 ± 0.085	18.371%	
	16 000	$(-634 \pm 40) \times 10^5$	1.80 ± 0.26		
	32 000	$(-221 \pm 37) \times 10^6$			

the autocorrelation times are much smaller†. They also increase more slowly with N; for O_1 we find $\tau_{\mathrm{int},O_1} \sim N^{\approx 0.3}$.

To eliminate these long autocorrelation times one must increase the frequency of the moves with the first points of the walk as pivots. We have thus modified the algorithm as follows. One iteration consists now of the following three moves:

- one move with pivot point in ω_1,
- one move with pivot point ω_k with k uniformly chosen in the interval $1 < k \leqslant 13$;
- one move with pivot point ω_k with k uniformly chosen in the interval $13 < k \leqslant N-1$.

With this improvement, the autocorrelation times are greatly reduced. Table 1 contains a comparison between autocorrelation times for the two algorithms for walks of length $N_{\mathrm{tot}} = 1000$. We observed sensible reductions of autocorrelation times for each observable, but the most impressive results are obtained for the observable $p_{\mathcal{R}}$, which denotes the fraction of walks that intersect the considered excluded set. To compare CPU times one should notice that one iteration of the improved algorithm takes three times the CPU time of an iteration of the standard algorithm. Thus in practice, use of the improved algorithm allowed us to gain a factor of 15–20 on $p_{\mathcal{R}}$ (although no improvement on the exponent p) and a factor of 1.5–2 on global observables such as O_1.

5. The results

We have studied SAWs of lengths $500 \leqslant N \leqslant 32\,000$. The number of iterations for each value of N is reported in table 2. The total simulation required 2500 hr of CPU on a AlphaStation 600 Mod 5/266. We have computed Δ studying the quantities we have previously discussed, whose leading behaviour for $N \to \infty$ is

$$\langle O_k\rangle_N = B_{\mathcal{R}}(k) N^{\sigma} \tag{34}$$

† When we speak of the autocorrelation time for O_1, we intend $\tau_{\mathrm{int},\mathcal{A}}$ as defined in (31), as this is the observable which controls the error on O_1.

Table 5. Two needles along two different axes. Here CL denotes the confidence level of the fit.

	Geometry 3				
	Cut	$\langle O\rangle \pm \delta\langle O\rangle$	$\sigma \pm \delta\sigma$	CL	
O_1	500	-1.6573 ± 0.0015	$0.392\,67 \pm 0.000\,44$	4×10^{-8}%	$\nu - \Delta$
	1 000	-2.1859 ± 0.0020	$0.390\,38 \pm 0.000\,60$	0.037%	$1 - \nu =$
	2 000	-2.8761 ± 0.0030	$0.387\,67 \pm 0.000\,92$	13.770%	0.4123 ± 0.0006
	4 000	-3.7761 ± 0.0048	$0.385\,0 \pm 0.001\,6$	59.748%	
	8 000	-4.9246 ± 0.0065	$0.387\,3 \pm 0.002\,9$	70.556%	
	16 000	-6.436 ± 0.016	$0.390\,1 \pm 0.008\,1$		
	32 000	-8.435 ± 0.042			
O_2	500	-10.696 ± 0.025	$0.971\,7 \pm 0.001\,0$	5×10^{-5}%	$2\nu - \Delta = 1$
	1 000	-20.740 ± 0.047	$0.976\,1 \pm 0.001\,3$	2.063%	
	2 000	-40.42 ± 0.11	$0.980\,9 \pm 0.002\,0$	55.682%	
	4 000	-79.86 ± 0.24	$0.981\,1 \pm 0.003\,4$	35.520%	
	8 000	-157.19 ± 0.45	$0.985\,9 \pm 0.005\,7$	31.462%	
	16 000	-309.9 ± 1.6	1.000 ± 0.015		
	32 000	-619.8 ± 5.6			
$\tilde{O}_2$	500	-0.1650 ± 0.0081	0.772 ± 0.036	5.684%	$2\nu - \Delta = 1$
	1 000	-0.276 ± 0.016	0.730 ± 0.057	4.327%	
	2 000	-0.572 ± 0.035	0.512 ± 0.092	89.526%	
	4 000	-0.819 ± 0.079	0.53 ± 0.18	74.224%	
	8 000	-1.07 ± 0.18	0.77 ± 0.43	63.693%	
	16 000	-2.02 ± 0.67	0.1 ± 1.4		
	32 000	-2.2 ± 2.0			
O_4	500	$(-166 \pm 12) \times 10^2$	2.244 ± 0.025	10.182%	$4\nu - \Delta =$
	1 000	$(-864 \pm 52) \times 10^2$	2.211 ± 0.032	16.821%	$1 + 2\nu =$
	2 000	$(-414 \pm 25) \times 10^3$	2.171 ± 0.046	17.299%	2.1754 ± 0.0012
	4 000	$(-214 \pm 12) \times 10^4$	2.071 ± 0.072	40.820%	
	8 000	$(-871 \pm 54) \times 10^4$	2.10 ± 0.14	18.912%	
	16 000	$(-409 \pm 42) \times 10^5$	1.56 ± 0.44		
	32 000	$(-120 \pm 34) \times 10^6$			

where $\sigma = k\nu - \Delta$, $k = 1, 2, 4$. We have performed standard power-law fits neglecting the next subleading terms. This introduces a systematic error which in our case could be particularly serious due to the small value of Δ. Indeed one expects corrections to (34) of the form $N^{k\nu-2\Delta}$ which decay very slowly and could thus give sizeable corrections even at the relatively large values of N that we use. To obtain an idea of the systematic error we have repeated the fits using each time only those values of N satisfying $N \geqslant N_{\rm cut}$. In this way one obtains different estimates which should converge to Δ as $N_{\rm cut}$ goes to infinity. If the different estimates are essentially independent of $N_{\rm cut}$ (within error bars) one can reasonably trust the estimate of Δ, otherwise one obtains an idea of the size of the systematic error.

We show the results of our fits for each geometry in tables 3–8. In the first column one can find the different values of $N_{\rm cut}$, the second column gives the raw Monte Carlo data, the third column gives the estimated value of the exponent and the the fourth column gives the confidence level of the fit. In the last column we report the 'classical prediction' for the exponent σ, obtained using (8). In the computation of the expectation values we used the

Table 6. Four needles in a plane. Here CL denotes the confidence level of the fit.

	Geometry 4				
	Cut	$\langle O\rangle \pm \delta\langle O\rangle$	$\sigma \pm \delta\sigma$	CL	
O_2	500	-25.876 ± 0.071	0.9439 ± 0.0012	10^{-7}%	$2\nu - \Delta = 1$
	1 000	-49.00 ± 0.13	0.9501 ± 0.0016	0.747%	
	2 000	-93.52 ± 0.29	0.9561 ± 0.0024	34.436%	
	4 000	-182.09 ± 0.63	0.9552 ± 0.0040	19.884%	
	8 000	-351.1 ± 1.2	0.9643 ± 0.0072	35.181%	
	16 000	-682.1 ± 4.1	0.981 ± 0.020		
	32 000	-1347 ± 17			
O_4	500	$(-518 \pm 13) \times 10^2$	2.1760 ± 0.0099	3.475%	$4\nu - \Delta$
	1 000	$(-2425 \pm 55) \times 10^2$	2.161 ± 0.013	6.562%	$1 + 2\nu =$
	2 000	$(-1104 \pm 27) \times 10^3$	2.142 ± 0.019	7.781%	2.1754 ± 0.0012
	4 000	$(-521 \pm 14) \times 10^4$	2.094 ± 0.031	24.042%	
	8 000	$(-2181 \pm 61) \times 10^4$	2.1083 ± 0.057	9.664%	
	16 000	$(-991 \pm 42) \times 10^5$	1.86 ± 0.16		
	32 000	$(-359 \pm 37) \times 10^6$			

Table 7. Three needles along three different axes. Here CL denotes the confidence level of the fit.

	Geometry 5				
	Cut	$\langle O\rangle \pm \delta\langle O\rangle$	$\sigma \pm \delta\sigma$	CL	
O_1	500	-1.8113 ± 0.0017	0.38443 ± 0.00045	13×10^{-10}%	$\nu - \Delta =$
	1 000	-2.3764 ± 0.0022	0.38193 ± 0.00061	0.012%	$1 - \nu =$
	2 000	-3.1097 ± 0.0034	0.37900 ± 0.00093	12.449%	0.4123 ± 0.0006
	4 000	-4.0587 ± 0.0053	0.3762 ± 0.0016	55.622%	
	8 000	-5.2613 ± 0.0073	0.3786 ± 0.0030	58.046%	
	16 000	-6.833 ± 0.016	0.3828 ± 0.0082		
	32 000	-8.909 ± 0.046			
$\tilde{O}_2$	500	-0.1892 ± 0.0088	0.763 ± 0.034	3.242%	$2\nu - \Delta = 1$
	1 000	-0.311 ± 0.017	0.732 ± 0.052	2.100%	
	2 000	-0.645 ± 0.038	0.518 ± 0.084	81.853%	
	4 000	-0.952 ± 0.086	0.50 ± 0.17	63.392%	
	8 000	-1.20 ± 0.17	0.79 ± 0.39	61.993%	
	16 000	-2.27 ± 0.66	0.2 ± 1.3		
	32 000	-2.5 ± 2.2			
O_4	500	$(-282 \pm 12) \times 10^2$	2.211 ± 0.016	5.575%	$4\nu - \Delta =$
	1 000	$(-1393 \pm 53) \times 10^2$	2.188 ± 0.021	10.689%	$1 + 2\nu =$
	2 000	$(-649 \pm 26) \times 10^3$	2.159 ± 0.030	11.283%	2.1754 ± 0.0012
	4 000	$(-321 \pm 13) \times 10^4$	2.088 ± 0.048	30.950%	
	8 000	$(-1334 \pm 54) \times 10^4$	2.103 ± 0.089	12.901%	
	16 000	$(-618 \pm 42) \times 10^5$	1.73 ± 0.26		
	32 000	$(-205 \pm 35) \times 10^6$			

estimate for ν given by [27]

$$\nu = 0.5877 \pm 0.0006. \tag{35}$$

Table 8. Six needles along the two directions of all the three axes. Here CL denotes the confidence level of the fit.

	Geometry 6				
	Cut	$\langle O\rangle \pm \delta\langle O\rangle$	$\sigma \pm \delta\sigma$	CL	
O_4	500	$(-787 \pm 16) \times 10^2$	2.1540 ± 0.0086	4.443%	$4\nu - \Delta =$
	1 000	$(-3606 \pm 67) \times 10^2$	2.141 ± 0.011	7.879%	$1 + 2\nu =$
	2 000	$(-1611 \pm 35) \times 10^3$	2.123 ± 0.017	9.185%	2.1754 ± 0.0012
	4 000	$(-746 \pm 17) \times 10^4$	2.078 ± 0.028	33.022%	
	8 000	$(-3093 \pm 76) \times 10^4$	2.097 ± 0.053	15.301%	
	16 000	$(-1382 \pm 56) \times 10^5$	1.89 ± 0.15		
	32 000	$(-513 \pm 50) \times 10^6$			

Let us now comment on the results. Let us consider first the observable O_1. Since the estimates for $N_{\rm cut} \geqslant 4000$ are essentially constant within error bars one could estimate

$$\sigma = \begin{cases} 0.396(3) & \text{for geometry 1} \\ 0.388(3) & \text{for geometry 3} \\ 0.379(3) & \text{for geometry 5.} \end{cases} \tag{36}$$

These estimates have very small statistical error bars. However, the fact that the estimates do not agree within the stated errors is a clear indication that there is a much larger error due to the neglected corrections to scaling. Indeed a closer look to the data shows that in all cases there is still an upward trend, although not statistically significant, as the change of σ is smaller than the error bars. It is thus more cautious to interpret the results for σ as lower bounds on the true value. Thus we estimate $\sigma \gtrsim 0.39 \pm 0.01$ and thus $\Delta \lesssim 0.20 \pm 0.01$.

Let us now consider the observable O_2. This quantity shows much larger corrections to scaling compared with the previous one: indeed in no case can we identify a region of $N_{\rm cut}$ where the estimates are constant. In all cases the estimates of σ clearly increase with $N_{\rm cut}$. Using the results with $N_{\rm cut} = 8000$ we have

$$\sigma \gtrsim \begin{cases} 0.991(5) & \text{for geometry 1} \\ 0.980(6) & \text{for geometry 2} \\ 0.986(6) & \text{for geometry 3} \\ 0.964(7) & \text{for geometry 4 .} \end{cases} \tag{37}$$

We conclude thus that $\sigma \gtrsim 0.99 \pm 0.01$ so that $\Delta \lesssim 0.19 \pm 0.01$.

Consider now the observable O_4. It has much larger errors than the two previous ones. Here we can only give a very rough estimate $\sigma \approx 2.10(10)$ so that $\Delta \approx 0.25(10)$.

Finally let us discuss the results for $\tilde{O}_2$. In this case the estimates of σ are much lower than expected and indeed for both geometries 3 and 5 they seem to indicate, although without much confidence, $\sigma \approx 0.5 \pm 0.2$. It thus appears that this observable does not couple to the leading operator breaking the rotational invariance. This fact can be proved rigorously for the ordinary random walk: in appendix A we show that for geometries 3 and 5 we have indeed

$$\langle \tilde{O}_2 \rangle_N = 0 \tag{38}$$

for all values of N. For the SAW $\langle \tilde{O}_2 \rangle_N \neq 0$; however, our data show that for this observable, in formula (7), not only A but also $B_{\mathcal{R}}$ vanishes. Thus, the study of $\langle \tilde{O}_2 \rangle_N$

Table 9. Probabilities of intersection $p_{\mathcal{R}}$ for the various geometries. Here CL denotes the confidence level of the fit used to determine Δ.

Geometry	Cut	$p_{\mathcal{R}} \pm \delta p_{\mathcal{R}}$	$\Delta \pm \delta\Delta$	CL
1	500	$0.182\,995 \pm 0.000\,067$	0.2150 ± 0.0064	74.926%
	1 000	$0.194\,002 \pm 0.000\,070$	0.215 ± 0.012	58.808%
	2 000	$0.203\,434 \pm 0.000\,089$	0.223 ± 0.026	40.621%
	4 000	$0.211\,73 \pm 0.000\,12$	0.16 ± 0.13	56.695%
	8 000	$0.218\,61 \pm 0.000\,14$		
	16 000	$0.224\,61 \pm 0.000\,27$		
	32 000	$0.230\,41 \pm 0.000\,58$		
2	500	$0.346\,24 \pm 0.000\,12$	0.2357 ± 0.0067	83.318%
	1 000	$0.364\,15 \pm 0.000\,12$	0.234 ± 0.013	69.572%
	2 000	$0.379\,28 \pm 0.000\,15$	0.237 ± 0.027	48.991%
	4 000	$0.392\,35 \pm 0.000\,19$	0.176 ± 0.052	61.677%
	8 000	$0.403\,09 \pm 0.000\,22$		
	16 000	$0.412\,35 \pm 0.000\,44$		
	32 000	$0.421\,16 \pm 0.000\,94$		
3	500	$0.334\,56 \pm 0.000\,11$	0.2276 ± 0.0063	74.457%
	1 000	$0.352\,09 \pm 0.000\,11$	0.226 ± 0.012	58.934%
	2 000	$0.366\,96 \pm 0.000\,14$	0.232 ± 0.026	39.799%
	4 000	$0.379\,93 \pm 0.000\,18$	0.168 ± 0.086	54.075%
	8 000	$0.390\,61 \pm 0.000\,21$		
	16 000	$0.399\,83 \pm 0.000\,41$		
	32 000	$0.408\,74 \pm 0.000\,88$		
4	500	$0.583\,02 \pm 0.000\,15$	0.2637 ± 0.0067	75.629%
	1 000	$0.605\,09 \pm 0.000\,15$	0.259 ± 0.013	64.062%
	2 000	$0.623\,32 \pm 0.000\,18$	0.258 ± 0.027	43.116%
	4 000	$0.638\,75 \pm 0.000\,23$	0.195 ± 0.064	55.552%
	8 000	$0.651\,23 \pm 0.000\,25$		
	16 000	$0.661\,82 \pm 0.000\,47$		
	32 000	$0.671\,8 \pm 0.001\,0$		
5	500	$0.460\,27 \pm 0.000\,13$	0.2397 ± 0.0063	72.307%
	1 000	$0.481\,13 \pm 0.000\,13$	0.236 ± 0.012	58.015%
	2 000	$0.498\,65 \pm 0.000\,16$	0.242 ± 0.025	38.594%
	4 000	$0.513\,80 \pm 0.000\,21$	0.177 ± 0.072	53.900%
	8 000	$0.526\,19 \pm 0.000\,24$		
	16 000	$0.536\,83 \pm 0.000\,46$		
	32 000	$0.547\,0 \pm 0.001\,0$		
6	500	$0.745\,26 \pm 0.000\,16$	0.2897 ± 0.0068	49.055%
	1 000	$0.764\,91 \pm 0.000\,14$	0.280 ± 0.012	49.324%
	2 000	$0.780\,69 \pm 0.000\,17$	0.276 ± 0.024	30.554%
	4 000	$0.793\,89 \pm 0.000\,19$	0.206 ± 0.052	57.904%
	8 000	$0.804\,32 \pm 0.000\,20$		
	16 000	$0.813\,12 \pm 0.000\,35$		
	32 000	$0.821\,26 \pm 0.000\,67$		

allows us to compute a new subleading exponent $\Delta' > \Delta$: from $\sigma \sim 0.5$ we would obtain $\Delta' \sim 0.7$. Notice, however, that the error bars are too big to really trust this estimate.

Let us now discuss the behaviour of the intersection probabilities $p_{\mathcal{R}}$. As discussed before, pure-dimensional arguments suggest that the probability of a SAW intersecting any one-dimensional set is vanishing in a three-dimensional space. This argument works of course in the *continuum* limit. For SAWs on the lattice this statement translates in the fact that given a SAW of length N, $\{\omega_i\}_{i=0,\ldots,N}$, and a one-dimensional set S such that ω_0 is at a distance of order N^{ν} from S, then the probability that the walk intersects S goes to zero for $N \to \infty$ as $N^{-\Delta}$. In our case $p_{\mathcal{R}}$ is, however, the probability that the SAW intersects a one-dimensional set $\mathcal{R}$ which is at a finite fixed distance from the origin of the walk. In this case we expect the intersection probability to tend to a constant as $N \to \infty$ and thus a behaviour of the form

$$p_{\mathcal{R}}(N) = p_{\mathcal{R}}(\infty) + \frac{b_{\mathcal{R}}}{N^{\Delta}}. \tag{39}$$

The results for $p_{\mathcal{R}}$ for the various geometries are reported in table 9, together with the estimates of Δ from a three-parameter fit of the form (39). The estimates indicate $\Delta = 0.23(3)$ except for the geometry 6 in which case one would derive a much higher value of Δ, $\Delta \approx 0.28$. These discrepancies should not, however, be taken seriously: fit (39) is very unstable in the presence of additional subleading corrections. To understand the size of the systematic error one should expect from fits of the form (39), we have performed the following test: we have considered O_1 and we have analysed the data as

$$\frac{\langle O_1 \rangle_N}{N^{\nu}} = a + bN^{-\Delta} \tag{40}$$

where we have used $\nu = 0.5877$. In all cases we have obtained estimates $\Delta \approx 0.16$–0.23 and moreover we have found a barely compatible with zero within error bars (for instance for the geometry 1, $N_{\mathrm{cut}} = 4000$, we have $a = (24 \pm 23) \times 10^{-4}$). Clearly the additional corrections still play an important role. It is, however, reassuring that the value of Δ is in essential agreement with what we expect.

6. Conclusions

In this paper we have studied the role played by one-dimensional vacancies in the critical behaviour of the three-dimensional SAW. As already pointed out in [1, 2] a new critical exponent arises. We have carefully checked that the exponent depends only on the dimensionality of the vacancies by verifying its independence from the shape of the excluded region: in particular, it does not depend on the discrete symmetry which the lattice has after the introduction of the excluded region.

We have given a geometrical argument to interpret the new exponent and we have thus derived a classical prediction for it. Of course we expect renormalization effects to change the classical formula: we will thus write

$$\Delta = 2\nu - 1 + \eta_{\mathcal{R}} \approx 0.175 + \eta_{\mathcal{R}}. \tag{41}$$

The quantity $\eta_{\mathcal{R}}$ is an anomalous dimension which is expected to be small. Our numerical data give

$$\Delta = 0.18 \pm 0.02 \tag{42}$$

so that $|\eta_{\mathcal{R}}| \lesssim 0.02$. The classical prediction, obtained by setting $\eta_{\mathcal{R}} = 0$ is thus a very good approximation.

Let us notice that our estimate of Δ is somewhat lower than the estimate of [1], $\Delta \approx 0.24$ and of [2], $\Delta \approx 0.217 \pm 0.013$. The origin of these discrepancies is probably in the neglected

additional corrections to scaling: the results of [1] are obtained from an exact enumeration and thus probe only very short walks, while the estimate of [2] comes from walks which have mainly $N \approx 1000$–4000. Here we use longer SAWs and a much higher statistics and thus we can do a much more detailed study of the role of the next subleading terms. We thus hope to have a better control of the additional corrections although it is conceivable that also our present estimate is systematically higher than the true result. We hope that our error bar, which we believe is very conservative, takes these systematic effects correctly into account.

Let us finally remark that all the arguments we have given are of extremely general nature and can thus be used for other systems and geometries.

Appendix A. Critical behaviour of random walks in the presence of $d_{\mathcal{R}}$-dimensional vacancies

Consider a d-dimensional lattice Ω and a region $\mathcal{R}$. Then let $c_N(x)$ be the number of ordinary random walks, starting from the origin and ending in x, that never intersect $\mathcal{R}$ except for $t = 0$. In this appendix we will derive a general integral equation for the generating function which can be solved exactly when $\mathcal{R}$ is a $d_{\mathcal{R}}$-dimensional hyperplane. In this way we will be able to check the computations of section 2.

Let us start from the recursion relations

$$\begin{aligned} &c_0(x) = \delta(x,0) \\ &c_N(x) = \sum_{i=1}^{d} [c_{N-1}(x+e_i) + c_{N-1}(x-e_i)] \left(1 - \sum_{\alpha\in\mathcal{R}} \delta(x,\alpha)\right) \qquad \text{for } N \geqslant 1 \end{aligned} \tag{A.1}$$

where e_i is the unit vector in the i-direction. Let us now introduce the generating function

$$G(x) = \sum_{N=0}^{\infty} \beta^N c_N(x) \tag{A.2}$$

and its Fourier transform $\hat{G}(q)$. It is then a simple matter to obtain the following equation

$$\hat{G}(q) = 1 + \beta \hat{G}(q)(2d - \hat{q}^2) - \beta \int_{-\pi}^{\pi} \frac{\mathrm{d}^d k}{(2\pi)^d} \hat{G}(k)(2d - \hat{k}^2) \sum_{\alpha\in\mathcal{R}} \mathrm{e}^{\mathrm{i}(k-q)\alpha} \tag{A.3}$$

where $\hat{q}_i = 2\sin(\frac{q_i}{2})$. We now define the free propagator which coincides (apart from a factor β) with the generating function for unconstrained random walks

$$D(q) = \frac{1}{m_0^2 + \hat{q}^2} = \frac{\beta}{1 - 2\beta \sum_{i=1}^{d} \cos q_i} \tag{A.4}$$

where $m_0^2 = \frac{1-2\beta d}{\beta}$. Then (A.3) can be rewritten as

$$\hat{G}(q) = \frac{1}{\beta} D(q) - D(q) \int_{-\pi}^{\pi} \frac{\mathrm{d}^d k}{(2\pi)^d} \hat{G}(k)(2d - \hat{k}^2) \sum_{\alpha\in\mathcal{R}} \mathrm{e}^{\mathrm{i}(k-q)\alpha}. \tag{A.5}$$

This equation is completely general and applies to any excluded region $\mathcal{R}$.

Let us now restrict ourselves to the case in which $\mathcal{R}$ is the $d_{\mathcal{R}}$-dimensional hyperplane given by the equations $x_{d_{\mathcal{R}}+1} = \cdots = x_d = 0$. If we now multiply (A.5) by $(2d - \hat{q}^2) \sum_{\eta\in\mathcal{R}} \mathrm{e}^{\mathrm{i}(q-k')\eta}$ and integrate over q, using the identity $2d - \hat{q}^2 = \frac{1}{\beta} - D(q)^{-1}$,

we obtain

$$\int_{-\pi}^{\pi}\frac{\mathrm{d}^d q}{(2\pi)^d}\hat{G}(q)(2d-\hat{q}^2)\sum_{\alpha\in\mathcal{R}}\mathrm{e}^{\mathrm{i}(q-k')\alpha}=\frac{1}{\beta}\left[1-\beta\left(\int_{-\pi}^{\pi}\frac{\mathrm{d}^d q}{(2\pi)^d}D(q)\sum_{\alpha\in\mathcal{R}}\mathrm{e}^{\mathrm{i}(q-k')\alpha}\right)^{-1}\right]. \tag{A.6}$$

Inserting it back into (A.5) we finally obtain

$$\hat{G}(q)=\frac{D(q)}{\int_{-\pi}^{\pi}\frac{\mathrm{d}^{\mathcal{D}_\mathcal{R}}k}{(2\pi)^{\mathcal{D}_\mathcal{R}}}D(q_1,\ldots,q_{d_\mathcal{R}},k_{d_\mathcal{R}+1},\ldots,k_d)} \tag{A.7}$$

where $\mathcal{D}_\mathcal{R}=d-d_\mathcal{R}$. It is easy to check that this solution has the correct properties. Indeed one can verify immediately that $G(x)=\delta_{x,0}$ whenever $x\in\mathcal{R}$. Notice finally that for $d_\mathcal{R}=0$ the solution does not become the standard solution for unconstrained random walks, but gives the generating function for random walks with the excluded origin.

Let us now consider the critical limit $m_0\to 0$ and let us define

$$\begin{aligned}I_\mathcal{R}(\hat{m}_0^2)&\equiv\int_{-\pi}^{\pi}\frac{\mathrm{d}^{\mathcal{D}_\mathcal{R}}k}{(2\pi)^{\mathcal{D}_\mathcal{R}}}D(q_1,\ldots,q_{d_\mathcal{R}},k_{d_\mathcal{R}+1},\ldots,k_d)\\&=\int_{-\pi}^{\pi}\frac{\mathrm{d}^{\mathcal{D}_\mathcal{R}}k}{(2\pi)^{\mathcal{D}_\mathcal{R}}}\frac{1}{\hat{m}_0^2+\hat{k}^2}\end{aligned} \tag{A.8}$$

where $\hat{m}_0^2=m_0^2+\hat{q}_\parallel^2$ and $q_\parallel=(q_1,\ldots,q_{d_\mathcal{R}},0,\ldots,0)$. The introduction of the excluded region will thus be relevant or irrelevant depending on the behaviour of $I(\hat{m}_0^2)$ for $\hat{m}_0\to 0$. If the limit exists the perturbation is irrelevant, while if the integral diverges the perturbation is relevant or marginal. This last case corresponds to $\mathcal{D}_\mathcal{R}=1,2$. For $\mathcal{D}_\mathcal{R}=1$, we have

$$I_\mathcal{R}(\hat{m}_0^2)=\frac{1}{\hat{m}_0\sqrt{\hat{m}_0^2+4}} \tag{A.9}$$

and the critical behaviour is drastically changed since

$$\hat{G}(q)=\frac{\sqrt{m_0^2+\hat{q}_\parallel^2}\sqrt{m_0^2+\hat{q}_\parallel^2+4}}{m_0^2+\hat{q}^2}. \tag{A.10}$$

In the critical limit we have

$$\hat{G}(q)=\frac{2\sqrt{m_0^2+{q_\parallel}^2}}{m_0^2+q^2}. \tag{A.11}$$

From this expression it is easy to verify that, for $N\to\infty$,

$$c_N\equiv\sum_x c_N(x)\approx\frac{2}{\sqrt{2\pi d}}(2d)^N N^{-1/2} \tag{A.12}$$

so that $\gamma=\frac{1}{2}$ which differs from the value of γ for random walks in free space, $\gamma=1$. Analogously we have

$$\langle x_1^2\rangle_N\approx\frac{N}{d} \tag{A.13}$$

$$\langle x_d^2\rangle_N\approx\frac{2N}{d}. \tag{A.14}$$

The exponent ν is not changed, but the amplitudes are, as expected, dependent on the direction and different from the value they assume in free space, $\langle x_1^2\rangle_N=\langle x_d^2\rangle_N=N/d$.

If $\mathcal{D}_{\mathcal{R}} = 2$, which, as we shall see, corresponds to a marginal operator, we have

$$I_{\mathcal{R}}(\hat{m}_0^2) = \frac{2}{\pi}\frac{1}{\hat{m}_0^2+4} K\left(\frac{4}{\hat{m}_0^2+4}\right) \tag{A.15}$$

where $K(z)$ is an elliptic integral. For $\hat{m}_0^2 \to 0$, $I_{\mathcal{R}}(\hat{m}_0^2)$ diverges logarithmically so that we obtain in the critical limit

$$\hat{G}(q) = -\frac{4\pi}{(m_0^2+q^2)\log[(m_0^2+q_\parallel^2)/32]}. \tag{A.16}$$

Thus, the propagator differs from the unperturbed one only by a logarithmic correction. From this expression we easily obtain

$$c_N \equiv \sum_x c_N(x) \sim \frac{(2d)^N}{\log N}. \tag{A.17}$$

Thus, in this case we have $\gamma = 1$ as for random walks in free space: however, an additional logarithmic correction appears as expected in the marginal case. Analogously we find

$$\langle x_1^2 - x_d^2 \rangle_N \sim \frac{N}{\log N}. \tag{A.18}$$

If now $\mathcal{D}_{\mathcal{R}} > 2$ $I_{\mathcal{R}}(\hat{m}_0^2)$ has a finite limit for $\hat{m}_0 \to 0$ so that in the critical limit

$$\hat{G}(q) = \frac{D(q)}{I_{\mathcal{R}}(0)}. \tag{A.19}$$

Thus $\hat{G}(q)$ is identical to the generating function of unconstrained random walks except for a multiplicative constant which is related to the total number of walks $c_N = \sum_x c_N(x)$. Indeed from (A.19) it follows that for large N

$$c_N \approx \frac{(2d)^N}{2d I_{\mathcal{R}}(0)} \tag{A.20}$$

so that $p_{\mathcal{R}}$, the probability that an unconstrained random walk intersects $\mathcal{R}$ is simply $1 - 1/(2d I_{\mathcal{R}}(0))$. It is easy to check that this probability tends to zero as $d \to \infty$ at $d_{\mathcal{R}}$ fixed. Indeed, let us compute the large-$\mathcal{D}_{\mathcal{R}}$ expansion of $I_{\mathcal{R}}(0)$: we start from the standard representation of $I_{\mathcal{R}}(m_0^2)$ in terms of Bessel functions:

$$I_{\mathcal{R}}(\hat{m}_0^2) = \int_0^\infty \mathrm{d}t\, \mathrm{e}^{-t(\hat{m}_0^2+2\mathcal{D}_{\mathcal{R}})} I_0^{\mathcal{D}_{\mathcal{R}}}(2t) \tag{A.21}$$

where $I_0(t)$ is the zeroth-order Bessel function of first kind. Expanding $I_0(t)$ around $t = 0$ we finally obtain

$$I_{\mathcal{R}}(\hat{m}_0^2) = \frac{1}{\hat{m}_0^2 + 2\mathcal{D}_{\mathcal{R}}} \sum_{n_1=0}^\infty \cdots \sum_{n_{\mathcal{D}_{\mathcal{R}}}=0}^\infty \frac{(2n_1+\cdots+2n_{\mathcal{D}_{\mathcal{R}}})!}{(n_1!\ldots n_{\mathcal{D}_{\mathcal{R}}}!)^2} \frac{1}{(\hat{m}_0^2+2\mathcal{D}_{\mathcal{R}})^{2(n_1+\cdots+n_{\mathcal{D}_{\mathcal{R}}})}} \tag{A.22}$$

so that, for $\mathcal{D}_{\mathcal{R}} \to \infty$,

$$I_{\mathcal{R}}(0) \approx \frac{1}{2\mathcal{D}_{\mathcal{R}}}\left(1 + \frac{1}{2\mathcal{D}_{\mathcal{R}}} + \frac{3}{4\mathcal{D}_{\mathcal{R}}^2} + \cdots\right). \tag{A.23}$$

It follows that for $d \to \infty$, $p_{\mathcal{R}} \approx (2d_{\mathcal{R}}+1)/(2d)$.

Let us now discuss the subleading corrections to (A.19). We need here the small-$\hat{m}_0^2$ expansion of $I(\hat{m}_0^2)$. We start from the well known asymptotic expansion for large t of the Bessel function $I_0(2t)$

$$I_0^{\mathcal{D}_{\mathcal{R}}}(2t) \approx \mathrm{e}^{2\mathcal{D}_{\mathcal{R}}t} \sum_{n=0}^\infty \frac{b_n(\mathcal{D}_{\mathcal{R}})}{(2t)^{\frac{\mathcal{D}_{\mathcal{R}}}{2}+n}}. \tag{A.24}$$

Using (A.21) we can rewrite our integral as

$$I_{\mathcal{R}}(\hat{m}_0^2) \approx \int_0^1 \mathrm{d}t\, \mathrm{e}^{-t\hat{m}_0^2}[\mathrm{e}^{-2t} I_0(2t)]^{\mathcal{D}_{\mathcal{R}}} + \int_1^\infty \mathrm{d}t\, \mathrm{e}^{-t\hat{m}_0^2}\left[(\mathrm{e}^{-2t} I_0(2t))^{\mathcal{D}_{\mathcal{R}}} - \sum_{n=0}^{\infty} \frac{b_n(\mathcal{D}_{\mathcal{R}})}{(2t)^{\frac{\mathcal{D}_{\mathcal{R}}}{2}+n}}\right] + \int_1^\infty \mathrm{d}t\, \mathrm{e}^{-t\hat{m}_0^2} \sum_{n=0}^{\infty} \frac{b_n(\mathcal{D}_{\mathcal{R}})}{(2t)^{\mathcal{D}_{\mathcal{R}}/2+n}}. \tag{A.25}$$

The first two integrals have a regular expansion in terms of powers of $\hat{m}_0^2$.

Let us now determine the behaviour in $\hat{m}_0^2$ of the generic term appearing in the series in the last term. Integrating by parts we obtain

$$\begin{aligned}\int_1^\infty \mathrm{d}t\, \mathrm{e}^{-t\hat{m}_0^2} \frac{b_n(\mathcal{D}_{\mathcal{R}})}{(2t)^{\mathcal{D}_{\mathcal{R}}/2+n}} &= \frac{\hat{m}_0^{\mathcal{D}_{\mathcal{R}}+2n-2}}{2^{\mathcal{D}_{\mathcal{R}}/2+n}} b_n(\mathcal{D}_{\mathcal{R}}) \int_{\hat{m}_0{}^2}^\infty \mathrm{d}\xi\, \frac{\mathrm{e}^{-\xi}}{\xi^{\mathcal{D}_{\mathcal{R}}/2+n}} \\ &= \frac{b_n(\mathcal{D}_{\mathcal{R}})}{2^{\mathcal{D}_{\mathcal{R}}/2+n}} \left\{\left[\sum_{l=1}^{g(k,n)} \hat{m}_0^{2l-2}(-1)^{l-1}\left(\prod_{i=1}^{l} \frac{1}{\mathcal{D}_{\mathcal{R}}/2+n-\mathrm{i}}\right)\right]\left[\sum_{s=0}^{\infty} \frac{(-1)^s}{s!}\hat{m}_0^{2s}\right]\right. \\ &\quad \left. +(-1)^{g(k,n)} \hat{m}_0^{\mathcal{D}_{\mathcal{R}}+2n-2} F(\hat{m}_0^2)\left(\prod_{i=1}^{g(k,n)} \frac{1}{\mathcal{D}_{\mathcal{R}}/2+n-\mathrm{i}}\right)\right\}\end{aligned} \tag{A.26}$$

where, for k integer,

$$g(k,n) = \begin{cases} k+n-1 & \text{if } \mathcal{D}_{\mathcal{R}} = 2k \\ k+n+1 & \text{if } \mathcal{D}_{\mathcal{R}} = 2k+1 \end{cases} \tag{A.27}$$

$$F(\hat{m}_0^2) = \begin{cases} -\mathrm{Ei}(-\hat{m}_0^2) = -\log \hat{m}_0^2 - \gamma_E - \displaystyle\sum_{k=1}^{\infty} \frac{(-1)^k \hat{m}_0^{2k}}{k\,k!} & \text{if } \mathcal{D}_{\mathcal{R}} = 2k \\ \dfrac{\sqrt{\pi}}{2} - \hat{m}_0^3 \displaystyle\sum_{k=0}^{\infty} \frac{(-1)^k \hat{m}_0^{2k}}{(k+\frac{3}{2})k!} & \text{if } \mathcal{D}_{\mathcal{R}} = 2k+1. \end{cases} \tag{A.28}$$

Here γ_E is the Euler–Mascheroni constant, $\gamma_E \approx 0.577\,215\,6649$. The whole integral can be represented in terms of $\hat{m}_0^2$ by

$$I_{\mathcal{R}}(\hat{m}_0^2) = \sum_{n=0}^{\infty} A_n \hat{m}_0^{2n} + \hat{m}_0^{\mathcal{D}_{\mathcal{R}}-2} C(\hat{m}_0^2). \tag{A.29}$$

A_n are suitable constants and $C(\hat{m}_0^2)$ is a function of $\hat{m}_0^2$ which is finite for $\hat{m}_0^2 \to 0$ for $\mathcal{D}_{\mathcal{R}}$ odd, diverging logarithmically for $\mathcal{D}_{\mathcal{R}}$ even. The second term in (A.29) represents the effect of the excluded region and corresponds to an exponent Δ

$$\Delta = \nu(\mathcal{D}_{\mathcal{R}} - 2) = \tfrac{1}{2}\mathcal{D}_{\mathcal{R}} - 1 \tag{A.30}$$

which agrees with our prediction.

To conclude this appendix let us prove a result for more general excluded regions which we will use in the main text. Let the excluded region be of the form $\mathcal{R} = \cup_{i=1}^{d} \mathcal{R}_i$ where $\mathcal{R}_i$ is some subset of points of the ith coordinate axis. If $i_1 \neq i_2 \ldots \neq i_n$, $2 \leqslant n \leqslant d$, then

$$\langle x_{i_1} x_{i_2} \ldots x_{i_n} \rangle_N = 0. \tag{A.31}$$

In particular, for geometries 3 and 5 we have $\langle \tilde{O}_2 \rangle_N = 0$.

To prove (A.31) consider (A.5), which, as we already said, is valid for general excluded regions $\mathcal{R}$. Using now

$$\frac{\partial}{\partial q_{i_1}}\frac{\partial}{\partial q_{i_2}}\cdots\frac{\partial}{\partial q_{i_n}}D(q)\bigg|_{q=0}=0 \tag{A.32}$$

$$\frac{\partial}{\partial q_{i_1}}\frac{\partial}{\partial q_{i_2}}\cdots\frac{\partial}{\partial q_{i_n}}\sum_{\alpha\in\mathcal{R}}\mathrm{e}^{\mathrm{i}(k-q)\alpha}=0 \tag{A.33}$$

for $i_1\neq i_2\ldots\neq i_n$, $2\leqslant n\leqslant d$, we obtain

$$\frac{\partial}{\partial q_{i_1}}\frac{\partial}{\partial q_{i_2}}\cdots\frac{\partial}{\partial q_{i_n}}\hat{G}(q)\bigg|_{q=0}=0 \tag{A.34}$$

from which (A.31) immediately follows.

Appendix B. Large-distance behaviour of the two-point function

In this appendix we will present some results which concern the three-dimensional self-avoiding walk with no excluded region and we will use it to discuss, along the lines of [31, 23], the behaviour of the two-point function $G(\boldsymbol{r};\beta)$ in the large-distance region $|r|\gtrsim R_e(\beta)$ where $R_e(\beta)$ is the mean end-to-end distance. Consider now the Fourier transform $\hat{G}(p;\beta)$; for $\beta\to\beta_c=1/\mu$ standard scaling theory predicts

$$\frac{\hat{G}(p;\beta)}{\hat{G}(0;\beta)}=\tilde{G}(q) \tag{B.1}$$

where $q=pR_e(\beta)/6$. An important characteristic of $\tilde{G}(q)$ is the fact that in the region $q^2\lesssim 1$, $\tilde{G}(q)$ is essentially a free-field propagator, i.e. it can be parametrized as

$$\tilde{G}(q)\approx\frac{1}{1+q^2}. \tag{B.2}$$

The deviations are small and can be parametrized by a $(q^2)^2$ term, i.e. by

$$\tilde{G}(q)\approx\frac{1}{1+q^2+b_2(q^2)^2}. \tag{B.3}$$

A strong-coupling (exact-enumeration) study [23] set a bound on b_2:

$$-3\times10^{-4}\lesssim b_2\lesssim 0. \tag{B.4}$$

The constant b_2 has also been computed [23] in the ϵ-expansion and in the expansion in fixed dimension with the result : $b_2=-3\times10^{-4}$.

Here we want to give a bound on b_2 using our Monte Carlo data. A simple computation gives

$$b_2=1-\frac{1}{2}\frac{\Gamma(\gamma)\Gamma(\gamma+4\nu)}{\Gamma(\gamma+2\nu)^2}Q \tag{B.5}$$

where

$$Q=\lim_{N\to\infty}Q_N\equiv\lim_{N\to\infty}\frac{\langle x^4+y^4+z^4\rangle_N}{\langle x^2+y^2+z^2\rangle_N^2}. \tag{B.6}$$

Our Monte Carlo estimates for Q_N are reported in table B1. It is evident that the data show strong corrections to scaling. To determine Q we have thus performed a fit of the form

$$Q_N=Q+\frac{A}{N^{\Delta}}. \tag{B.7}$$

Table B1. Mean values for SAWs in the absence of any excluded region. (x, y, z) are the coordinates of the endpoint of the walk.

N	$\langle x^2+y^2+z^2\rangle_N$	$\langle x^4+y^4+z^4\rangle_N$	Q_N
500	$1\,785.8 \pm 1.1$	$(28\,727 \pm 38) \times 10^2$	$0.900\,78 \pm 0.000\,46$
1 000	$4\,051.8 \pm 2.0$	$(14\,826 \pm 16) \times 10^3$	$0.903\,09 \pm 0.000\,39$
2 000	$9\,167.4 \pm 4.4$	$(76\,027 \pm 81) \times 10^3$	$0.904\,64 \pm 0.000\,38$
4 000	$20\,752.9 \pm 9.4$	$(38\,994 \pm 39) \times 10^4$	$0.905\,39 \pm 0.000\,36$
8 000	$46\,995 \pm 18$	$(20\,020 \pm 17) \times 10^5$	$0.906\,49 \pm 0.000\,32$
16 000	$106\,166 \pm 60$	$(10\,222 \pm 13) \times 10^6$	$0.906\,92 \pm 0.000\,47$
32 000	$240\,356 \pm 221$	$(5\,247 \pm 11) \times 10^7$	$0.908\,29 \pm 0.000\,78$

We find

$$Q = 0.9091 \pm 0.0016 \tag{B.8}$$

$$\Delta = 0.41 \pm 0.16 \tag{B.9}$$

$$\chi^2 = 1.77 \qquad (4 \text{ degrees of freedom}). \tag{B.10}$$

The value of Δ is in agreement with the estimates of [27]. Using for γ the value [32] $\gamma = 1.1575(6)$ we finally obtain

$$b_2 = -(13 \pm 17) \times 10^{-4}. \tag{B.11}$$

Our Monte Carlo data confirm the fact that b_2 is extremely small although we are unable to compute the actual value.

On the other hand, we can use (B.4) and (B.5) together with the estimates of γ and ν to obtain an estimate of Q. We obtain $Q = 0.9082(11)$.

References

[1] Considine D and Redner S 1989 *J. Phys. A: Math. Gen.* **22** 1621
[2] Caracciolo S, Ferraro G and Pelissetto A 1991 *J. Phys. A: Math. Gen.* **24** 3625
[3] Grassberger P 1993 *J. Phys. A: Math. Gen.* **26** 2769
[4] Daoud M, Cotton J P, Farnoux B, Jannink G, Sarma G, Benoit H, Duplessix R, Picot C and de Gennes P G 1975 *Macromolecules* **8** 804
[5] des Cloizeaux J 1975 *J. Physique* **36** 281
[6] Emery V J 1975 *Phys. Rev.* B **11** 239
[7] Aragão de Carvalho C, Caracciolo S and Fröhlich J 1983 *Nucl. Phys.* B **215** 209
[8] Fernández R, Fröhlich J and Sokal A D 1992 Random walks, critical phenomena, and triviality in quantum field theory *Text and Monographs in Physics* (Berlin: Springer)
[9] des Cloizeaux J and Jannink G J 1990 *Polymers in Solution: Their Modelling and Structure* (Oxford: Clarendon)
[10] Hammersley J M and Whittington S G 1985 *J. Phys. A: Math. Gen.* **18** 101
[11] Wegner F 1972 *Phys. Rev.* B **5** 4529
[12] Cardy J L and Redner S 1984 *J. Phys. A: Math. Gen.* **17** L933
[13] Bariev R Z 1979 *Zh. Eksp. Teor. Fiz.* **77** 1217
Bariev R Z 1979 *Sov. Phys.—JETP* **50** 613 (Engl. Transl.)
[14] Eisenriegler E and Burkhardt T 1981 *Phys. Rev.* B **24** 1236
[15] Symanzik K 1969 *Proc. Int. School of Physics 'Enrico Fermi' (Varenna Course XLV)* ed R Jost (New York: Academic)
[16] Fröhlich J 1982 *Nucl. Phys.* B **200** 281
[17] Parisi G 1979 *Phys. Lett.* **81B** 357
[18] Fisher M E 1984 *J. Stat. Phys.* **34** 665
[19] Huse D A and Fisher M E 1984 *Phys. Rev.* B **29** 239

[20] Mukherji S and Bhattacharjee S M 1995 *J. Phys. A: Math. Gen.* **26** L1139
Mukherji S and Bhattacharjee S M 1995 *J. Phys. A: Math. Gen.* **28** 4668
Mukherji S and Bhattacharjee S M 1993 *Phys. Rev.* E **48** 3427
Mukherji S and Bhattacharjee S M 1995 *Phys. Rev.* E **52** 3301
[21] Essam J W and Guttmann A J 1995 *Phys. Rev.* E **52** 5849
[22] Caracciolo S, Guttmann A, Li B, Pelissetto A and Sokal A D unpublished
[23] Campostrini M, Pelissetto A, Rossi P and Vicari E *Preprint* cond-mat/9612164 to appear in *Europhys. Lett.*
[24] Baker G A Jr, Nickel B G and Meiron D I 1978 *Phys. Rev.* B **17** 1365
[25] Le Guillou J C and Zinn-Justin J 1980 *Phys. Rev.* B **21** 3976
[26] Majid I, Djordjevic Z V and Stanley H E 1983 *Phys. Rev. Lett.* **51** 1282
[27] Li B, Madras N and Sokal A D 1995 *J. Stat. Phys.* **80** 661
[28] Madras N and Sokal A D 1988 *J. Stat. Phys.* **50** 109
[29] Lal M 1969 *Mol. Phys.* **17** 57
[30] MacDonald B, Jan N, Hunter D L and Steinitz M O 1985 *J. Phys. A: Math. Gen.* **18** 2627
[31] Fisher M E and Aharony A A 1973 *Phys. Rev. Lett.* **31** 1238
Fisher M E and Aharony A A 1974 *Phys. Rev.* B **7** 2818
[32] Caracciolo S, Causo M S and Pelissetto A High-precision determination of the critical exponent γ for self-avoiding walks *Preprint* SNS/PH/1997-002, cond-mat/9703250